Synthesis, Structure, and Stereodynamics of an *N,N*-Chiral "Proton Sponge"

Jonathan P. H. Charmant,[a] Guy C. Lloyd-Jones,*[a] Torren M. Peakman,[a] and Robert L. Woodward[a]

Keywords: Proton Sponges / *N*-Chirality / Isotopic labelling / Stereodynamics / NMR

1,8-Bis(*N*-benzyl-*N*-methylamino)naphthalene (**2**) and its hydrogen iodide salt [**2**H]$^+$[I]$^-$ were synthesised from 1,8-diaminonaphthalene. The thermodynamic diastereomer ratios of (**2**) and [**2**H]$^+$ in [D$_7$]DMF are 73.4:26.6 and 89.7:10.3 respectively at 293 K. The solid state structures of the major *dl*-(R_NR_N/S_NS_N) diastereomers were determined by single crystal X-ray diffraction. The minor diastereomers were shown to be the *meso*-(R_NS_N) forms by performing ^{1}H-NMR NOE studies on isotopically desymmetrized 1-(*N*-benzyl-*N*-[^{13}C]-methylamino)-8-(*N*′-benzyl-*N*′-methylamino)naphthalene [^{13}C]-**2** and the salt [^{13}C]-[**2**H]$^+$. In [D$_7$]DMF at 298 K, the *meso* form of the free base **2** is 0.6 (± 0.07) kcal·mol^{-1} less stable than the *dl* form ($\Delta H°$ = –0.64 (±0.03) kcal·mol^{-1}; $\Delta S°$ = –0.18 (±0.13) cal·K^{-1}mol^{-1}) and the activation barriers for interconversion are ca. 14.2 (±0.4) and 14.8 (±0.4) kcal·mol^{-1} respectively. The effect of solvent polarity on the entropy and enthalpy change on approach to the transition state was studied. An approximate correlation with the solvent dielectric constant was found for both $\Delta H^{\ddagger}$ and $\Delta S^{\ddagger}$ and this may be ascribed to the development of a net dipole in the transition state due to substantially different hybridisation and geometry at the two nitrogen centres.

Introduction

Although 1,8-bis(*N*,*N*-dimethylamino)naphthalene **1** had been known since 1941,[1] it was not until 1968 that its remarkable basicity was realised by Alder et al.[2] The unusual properties of **1**, led to the name "proton-sponge", by which it and compounds with analogous properties are now routinely called. The unusual and useful properties of the first generation proton sponges led to the design and development of second and third generation proton sponges by Staab et al.[3] However, the first generation proton sponges continue to generate interest.[4] Alder et al. and Hibbert et al. contributed extensively to the physical and synthetic chemistry of the first generation proton sponges[5] which are characterised by their high pK_a values (ca. 12−17) and "sluggish" behaviour: they are very poor nucleophiles and are protonated-deprotonated slowly.[6] Furthermore, once protonated they are very resistant to further protonation (Δ[pKa_1 pKa_2] ca. 20). Many novel first generation proton sponges (i.e. those based on a 1,8-diaminonaphthalene skeleton) have been reported − the area has recently been reviewed by Pozharskii.[7]

We are currently engaged in the synthesis and stereodynamics of chiral first generation proton sponges and in doing so have been studying [**2**H]$^+$[I]$^-$.[8] This salt, which has a stereogenic centre at both nitrogen atoms, exists as three stereoisomers: an enantiomeric and C_2 symmetric pair: [(R_NR_N/S_NS_N)-**2**H]$^+$ ("[*dl*]-[**2**H]$^+$") and an achiral form [(R_NS_N)-**2**H]$^+$ ("[*meso*]-[**2**H]$^+$"). Because of protonation, the two amine stereogenic centres in [**2**H]$^+$ are "locked"[9] together through hydrogen bonding.[10] Herein we report in full on the synthesis, structure, and stereodynamics of **2** and its protonated form.[11]

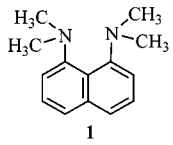

1

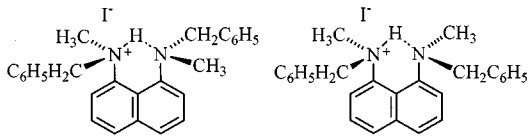

(±)-(dl)-[**2**H]$^+$[I]$^-$ [meso]-[**2**H]$^+$[I]$^-$

Results and Discussion

Synthesis and Solid-State Structures of Protonated and Free Base Forms of *N,N*-Chiral Proton Sponge 2

The synthesis of [**2**H]$^+$[I]$^-$ was readily achieved via two complementary routes that start from the readily prepared 9-BBN compound **3**,[12] and differ only in the order of alkylation. Thus, either dibenzylation followed by two-step dimethylation or dimethylation followed by two-step dibenzylation afforded the protonated form of **2** in fair to good yield − see Scheme 1.

The use of **3**, as reported by Kol et al.,[12] proved essential to attain the required regioselectivity in the first dialkylation step. The intermediate dialkylated 9-BBN-diaminonaphthalenes were hydrolysed with aqueous acid to afford dibenzylated **4** and dimethylated **5**. On reflux in THF with excess alkyl iodide and NaH, **4** and **5** were cleanly monoalkylated.[13] We currently favour the rationale that further methylation/benzylation of the anion (via N−H depro-

[a] School of Chemistry, University of Bristol, Cantock's Close, Bristol BS8 1TS, UK
Fax: (internat.) + 44-117/929-8611
E-mail: guy.lloyd-jones@bris.ac.uk

 © WILEY-VCH Verlag GmbH, D-69451 Weinheim, 1999 1434−193X/99/1010−2501 $ 17.50+.50/0

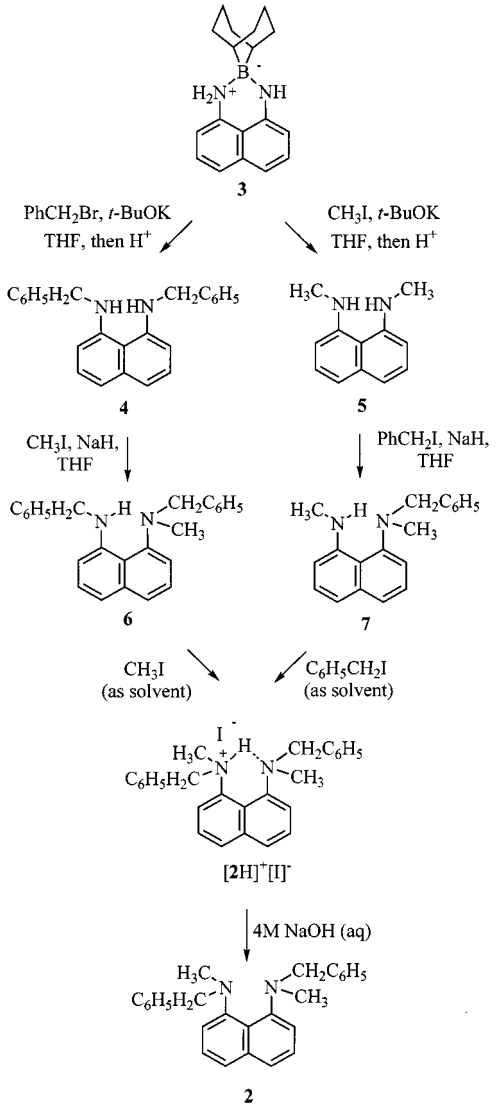

Scheme 1. The two routes employed in the synthesis of **2**

tonation by NaH) of **6** or **7** is slow since both reactions generate the proton sponge **2** in which there is substantial steric strain. Consistent with this explanation, simply dissolving neutral **6** in MeI and **7** in BnI resulted in smooth alkylation reactions to give $[\mathbf{2H}]^+[I]^-$ in which the steric strain present in **2** is relieved by protonation and thus the strain developed on approach to the transition state is lower than that induced on alkylation of the anions.

The non-protonated ("free base") form of the proton sponge **2** was generated by partitioning $[\mathbf{2H}]^+[I]^-$ between CH_2Cl_2 and 4 M aqueous NaOH.[14] Evaporation of the CH_2Cl_2 phase afforded the sesquihydrate of **2** as an analytically pure white powder. Good quality, anhydrous crystals of **2** were obtained on cooling toluene solutions of **2** to $-20°C$ – the single crystal X-ray structure is presented in Figure 1 (right hand structure). This structure may be compared with the single crystal structure X-ray structure of [*dl*]-$[\mathbf{2H}]^+[I]^-$ (left hand structure) which we have already reported.[8] Notably, both $[\mathbf{2H}]^+[I]^-$ and **2** crystallised as their [*dl*] forms with heterochiral unit cells.

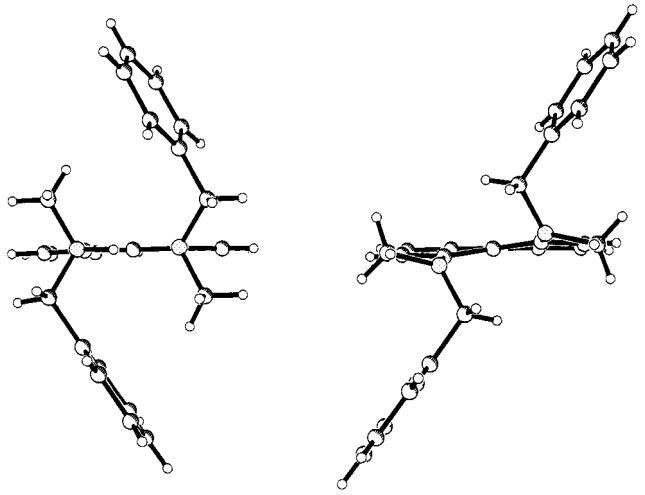

Figure 1. Single crystal X-ray structure of [*dl*]-$[\mathbf{2H}]^+$ (left hand structure) and **2** (right hand structure) both viewed along the naphthalene plane, with C(1), C(9), and C(8) at the front. The structure of [*dl*]-$[\mathbf{2H}]^+$ has been reported earlier (see ref.[8]). Crystallographic data for **2** has been deposited with the Cambridge Crystallographic Data Centre as supplementary publication no. CCDC-116496.

The single crystal structure determination carried out for **2** reveals a molecule with a heavily distorted naphthalene ring system. The nitrogen bound carbons lie 0.16 Å below and 0.14 Å above the ideal plane. This allows the two nitrogen atoms to separate to a distance of 2.81 Å, some 0.16 Å further apart than in the protonated derivative $[\mathbf{2H}]^+[I]^-$ in which there is no significant deviation from planarity within the naphthalene ring system. In the solid state, the free base **2** has its phenyl groups gauche with respect to the methyl groups when viewed along the CH_2-N bonds (torsion angles $-54.9°$ and $57.9°$). This is in contrast to the situation for $[\mathbf{2H}]^+[I]^-$ where corresponding torsion angles of $-163.8°$ and $-168.8°$ show these groups to have an approximately *anti*-conformation.

Structure and Reactivity of Precursor 6 – nOe Studies and Reaction with MeI

In order to study the methylation of **6**, which affords [*dl*]-$[\mathbf{2H}]^+[I]^-$ and [*meso*]-$[\mathbf{2H}]^+[I]^-$, we analysed both the geometry of **6** (as inferred by NMR studies in C_6D_6) and the rate of its reaction with methyliodide.

Both the ^{1}H- and ^{13}C-NMR chemical shifts of **6** (Figure 2) give some clue as to the geometry and extent of lone-pair delocalisation at the two, very different, nitrogen centres.

The upfield ^{13}C- and ^{1}H-NMR shifts at C(7)-H (δ_C 104.8, δ_H 6.52) are induced by shielding. This, together with the deshielded NH proton (δ_H 9.74) is indicative of trigonal geometry at the nitrogen attached to C(8) with extensive lone pair delocalisation into the aromatic ring. In stark contrast, the ^{13}C-/^{1}H-NMR chemical shifts at C(1), C(2)-H, C(3)-H, and C(4)-H are consistent with a pyramidal nitro-

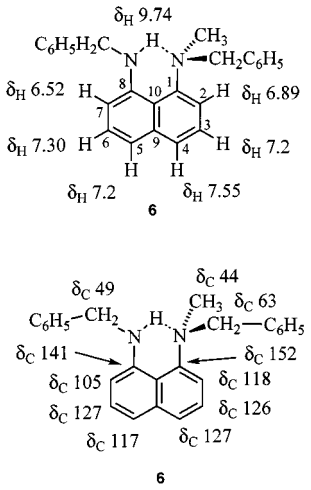

Figure 2. Selected data from the ^{1}H NMR (C_6D_6, 300 MHz, 21°C, TMS) and $^{13}C\{^1H\}$ NMR (C_6D_6, 75 MHz, 21°C, C_6D_6) spectra of diamine **6**, which support the notion of trigonal geometry at the C(8)-amino group and tetrahedral geometry at the C(1)-amino group

gen centre at C(1) and a resultant lack of delocalisation of the nitrogen lone pair into the aromatic system.

Further structural information was obtained by NOE difference spectroscopy and some selected results are presented in Figure 3 (**6**A and **6**B). A 16.8% NOE was observed at C(7)-H on irradiation of the benzylic protons of the $PhCH_2NH$ unit (Figure 3, **6**A), whilst negligible NOE was observed on irradiation of the N−H proton − although this did cause a 5.6% NOE at the benzylic protons indicating some freedom of rotation about the N−benzyl bond. The large (16.8%) NOE at C(7)-H further supports the assignment of trigonal geometry at the C(8)-NH centre and may be compared to the 9.2% and 6.1% NOE values observed at C(2)-H on irradiation of the benzyl and methyl protons of the $PhCH_2NMe$ unit (**6**A and **6**B respectively). These values support assignment of tetrahedral geometry at the C(1)-N centre and also suggest that in the time average population, the benzyl group is more proximal than the methyl group to C(2)-H. However, moderate Overhauser enhancements (3.2 and 3.1%) were also observed at the ortho and meta protons of the phenyl ring of the C(8) $PhCH_2NH$ unit (Figure 3, **6**B) which indicate that there is some freedom of rotation about the C(1)−N bond − in contrast to the restricted rotation around the C(8)−N bond due to lone-pair delocalisation.

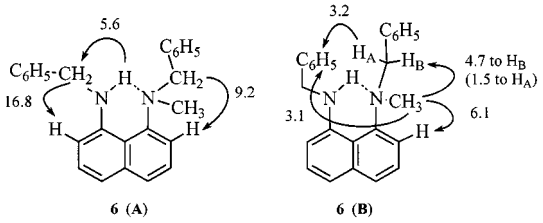

Figure 3. Selected NOE values (%) (by ^{1}H NMR NOE difference spectroscopy in C_6D_6 at 400 MHz and 21°C) for **6**

The various conformations of **6** at C(1) may be induced by a combination of two effects, firstly a steric inhibition of resonance caused by the steric bulk of the nitrogen centre at C(8) and secondly the availability of a hydrogen for H-bonding at the same centre. We therefore favour a model in which freedom of rotation about the C(1)−N bond is somewhat restricted by hydrogen bonding [i.e. C(8)−NH···N−C(1)] and this results in a time-average population that resides between the two *limiting* structures [**6***endo*] and [**6***exo*] in which the benzyl group at C(1)−N may be close to or orthogonal to the naphthalene ring − Figure 4.

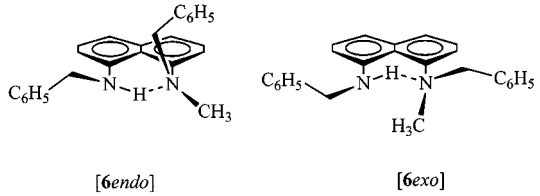

Figure 4. Two limiting conformers about C(1)-N, namely [**6***endo*] and [**6***exo*], in which the benzyl group at the pyramidal hydrogen bonded nitrogen centre may be close to or orthogonal to the naphthalene ring. The dominant conformer is considered to be [**6***exo*] based on selected Overhauser enhancements (see Figure 3).

Based on the Overhauser enhancements, the time-average population is closer to [**6***exo*] than [**6***endo*]. However, whether [**6***endo*] and [**6***exo*] are discrete species below the NMR time scale is not clear. Nonetheless, the primary process that effects conformational freedom between these extremes does not involve a rotation-inversion via passage of either the Me or the Bn groups through the plane of the naphthalene ring, at a rate faster than the NMR time scale. This conclusion is supported by the observation of a well resolved AB spin system [$\Delta\delta$(400 MHz) = 152 Hz; ^2J = 12.9 Hz] arising from the diastereotopic benzylic protons (H_A and H_B) of the C−N−C(1) nitrogen centre and the very different Overhauser enhancements (4.7 versus 1.5%, Figure 3, **6**B) observed on irradiation of the methyl group.

Diamine **6** proved quite air-sensitive in $CDCl_3$ and a deep brown colouration developed at the solvent-air interface. The ^{1}H-NMR spectrum displayed extensive broadening of the benzylic and NH protons on the C(8)-amino group as well as C(7)-H. A solution of **6** that had been prepared with $CDCl_3$ pre-filtered through alumina and then degassed did not discolour or display line broadening. On deliberate addition of 5 mol% O_2 a brown colouration developed and line broadening was observed in the ^{1}H-NMR spectrum − again only at the $PhCH_2NH$ unit and C(7)-H. These results may be explained by formation of a trace amount of paramagnetic species by O_2-induced loss of one electron from the trigonal nitrogen lone pair system. The resulting paramagnetic radical cation would induce localised line-broadening. Rapid intermolecular electron transfer between **6** and [$\mathbf{6}^{\bullet+}$] would then result in time-averaged broadening in all molecules of **6**. Analogous air sensitivity was not observed in C_6D_6 and therefore an acidic or polar medium appears necessary for this aerobic oxidation process.

The methylation of **6** to afford $[\mathbf{2H}]^+[I]^-$ occurs cleanly on dissolving **6** in methyliodide. To study the rate we employed CD_3I as both reactant and ^{1}H NMR solvent. The

single CH_3 groups in both **6** and $[[D_3]\text{-}\mathbf{2H}]^+[I]^-$ proved to have sharp signals suitable for integration and we were thus able to follow the rate of formation of $[[D_3]\text{-}\mathbf{2H}]^+[I]^-$, as well as being able to monitor the diastereomeric ratio of $[[D_3]\text{-}\mathbf{2H}]^+[I]^-$ through the reaction. To avoid the potential inaccuracies arising from crystallisation of $[[D_3]\text{-}\mathbf{2H}]^+[I]^-$ during the kinetics runs, the reactions were run at 8-fold dilution ($[\mathbf{6}]_{init}$ = 0.057 M) and kinetics obtained during the first 25% of reaction. The diastereomer ratio of $[\mathbf{2H}]^+[I]^-$ was constant (88.5:11.5) throughout this period. After ca. 25% conversion, the solubility limit of the product was reached and crystals of $[[D_3]\text{-}\mathbf{2H}]^+[I]^-$ appeared. Contrary to the expected pseudo first order kinetics (i.e. $d[\mathbf{6}]/dt = k[\mathbf{6}][CD_3I] \approx k'[\mathbf{6}]$), pseudo zero order kinetics were observed: ($d[\mathbf{6}]/dt = k[CD_3I] \approx k' = 0.3\cdot10^{-6}$ Ms^{-1}, r^2 = 0.995). The reaction, which occurs in a low polarity medium, must therefore require catalytic activation of the CD_3I. Since trace quantities of iodine are a common impurity in methyliodide, we suspected that iodine may function as such a catalyst by forming CD_3I_3 which on reaction with **6** would give $[[D_3]\text{-}\mathbf{2H}]^+[I_3]^-$ followed by dissociation of $[I_3]^-$ to I_2 and I^- thereby regenerating the catalyst. However, although addition of small quantities of I_2 resulted in large rate accelerations, the effect was stoichiometric. Thus far we have been unable to identify the catalyst.

There have been a number of measurements/calculations of the hydrogen-bond strength in $[\mathbf{1H}]^+$ the protonated form of the archetypal proton sponge 1,8-bis(dimethylamino)naphthalene **1**. These have ranged from 7 to 20 kcal·mol^{-1}.[10] It was expected that the strength of the H-bond would be such that the stereostructures of $[\mathbf{2H}]^+[I]^-$ would be "locked" at room temperature and thus would have half-lifes towards epimerisation in the region of weeks or years. It was therefore initially assumed that the 88.5:11.5 diastereomer ratio of $[dl]\text{-}[\mathbf{2H}]^+[I]^-$ to $[meso]\text{-}[\mathbf{2H}]^+[I]^-$obtained on methylation of **6** reflected the kinetic selectivity of the reaction. To explain this selectivity we considered the two diastereofaces available for methylation of **6** (via the more dominant [**6***exo*] conformer). The methyl group on the C(1)-N centre shields the back face of the lone pair at the C(8)-N centre and attack by MeI would therefore occur on the opposite face [*syn* to the benzyl group at C(1)-N] and thus give rise to an excess of $[dl]\text{-}[\mathbf{2H}]^+[I]^-$ over $[meso]\text{-}[\mathbf{2H}]^+[I]^-$ − Figure 5.

To test our model we prepared **7** (Scheme 1). The same arguments apply to rotation about C(1)−N in **7** as they do for **6** and [**7***exo*] was therefore assumed to be the closesr limiting structure to the time-average population of **7**. We thus supposed that attack by benzyliodide would occur *syn* to benzyl in [**7***exo*] to give rise to the $[meso]\text{-}[\mathbf{2H}]^+[I]^-$ isomer in excess over the $[dl]\text{-}[\mathbf{2H}]^+[I]^-$. To our surprise, ^{1}H-NMR analysis of a CD_2Cl_2 solution of $[\mathbf{2H}]^+[I]^-$ that crystallised from the reaction of **7** with benzyliodide indicated exactly the same ratio as obtained by the methylation of **6** (i.e. $[dl]\text{-}[\mathbf{2H}]^+[I]^-$ to $[meso]\text{-}[\mathbf{2H}]^+[I]^-$ = 88.5:11.5). It then became clear that $[\mathbf{2H}]^+[I]^-$ must be equilibrating in CD_2Cl_2 solution − indeed, large single crystals of pure $[dl]\text{-}[\mathbf{2H}]^+[I]^-$ were dissolved in CD_2Cl_2 at 25°C and reproducibly gave an 88.5:11.5 ratio of *dl*/*meso* diastereomers on ^{1}H-NMR analysis within 10 minutes in solution. Thus, although the rate of equilibration of *meso* and *dl* isomers of $[\mathbf{2H}]^+[I]^-$ is much slower than the NMR time scale it is fast at the real time-scale. The constant ratio of $[dl]\text{-}[\mathbf{2H}]^+[I]^-$ to $[meso]\text{-}[\mathbf{2H}]^+[I]^-$ (88.5:11.5) that was observed during reaction of **6** with CD_3I is therefore the thermodynamic product ratio. Whether this is identical with the kinetic selectivity ratio is hard to acertain since the rate of equilibration of $[dl]\text{-}[\mathbf{2H}]^+[I]^-$ and $[meso]\text{-}[\mathbf{2H}]^+[I]^-$ is many orders of magnitude greater[11] than the rate of their generation from **6** and CD_3I.

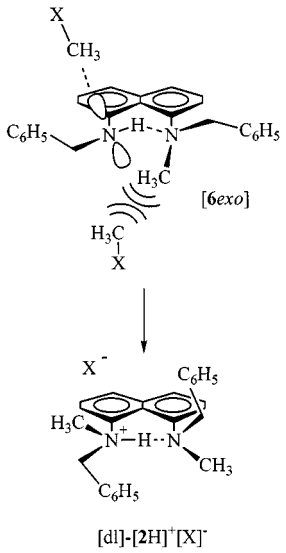

Figure 5. Possible mechanism resulting in kinetic-[*dl*]-selectivity in the methylation of **6**. *Note*: Diastereomers of $[\mathbf{2H}]^+$ interconvert at the real timescale in CH_3I and thus the methylation product $[\mathbf{2H}]^+$ is obtained with thermodynamic control and not kinetic control.

Solution Structures of $[\mathbf{2H}]^+$ and 2 − Preparation of ^{13}C-Labelled Proton Sponges

Since $[dl]\text{-}[\mathbf{2H}]^+[I]^-$ and $[meso]\text{-}[\mathbf{2H}]^+[I]^-$ equilibrate in CD_2Cl_2 solution and both isomers gave near identical NMR spectra but with small differences in chemical shift, we were unable to confidently assign the structures by routine ^{1}H or ^{13}C NMR. This problem is caused by the rotational and mirror plane symmetry in $[dl]\text{-}[\mathbf{2H}]^+[I]^-$ and $[meso]\text{-}[\mathbf{2H}]^+[I]^-$ respectively. To overcome this we prepared isotopically desymmetrised samples of $[\mathbf{2H}]^+[I]^-$ by methylating **4** with $^{13}CH_3I$ (91.4 and 99% ^{13}C)/NaH and dissolving the resultant ^{13}C-**6** in $^{12}CH_3I$ (natural abundance i.e. 98.9% ^{12}C). We were then able to perform ^{1}H-NMR studies on $[dl]\text{-}[^{13}\text{C-}\mathbf{2H}]^+$ and $[meso]\text{-}[^{13}\text{C-}\mathbf{2H}]^+$ isomers of $[^{13}\text{C-}\mathbf{2H}]^+[I]^-$ by exploiting the 150 Hz $^1J_{CH}$ coupling. This allowed us to selectively irradiate one of the ^{13}C or the ^{12}C methyl groups and observe the resultant NOE at the other. Clear evidence that the minor isomer is the [*meso*]-form came from the average 0.35% NOE observed at either methyl group on irradiation of its isotopomer.[8] These Overhauser enhancements were not observed in the major and

thus [*dl*]-isomer.[15] An identical sequence of NOE experiments was performed on the free base equilibrium mixture of [*dl*]-[^{13}C-**2**] and [*meso*]-[^{13}C-**2**]. Unfortunately, Overhauser enhancements were not observed between the protons of the ^{13}C and ^{12}C methyl groups − even when measurements were made at −30°C. However, the enhancements observed at the benzylic sites on irradiation of the ^{12}C methyl group were very different between the two isomers − Figure 6.

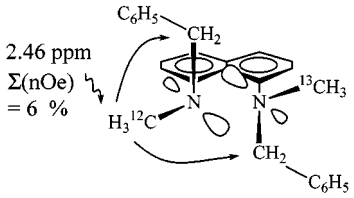

[^{13}C$_1$]-[dl]-(R_NR_N)/(S_NS_N)-**2**

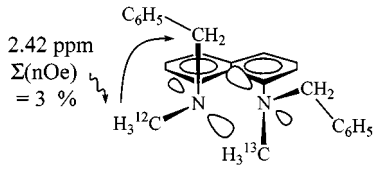

[^{13}C$_1$]-[meso]-(R_NS_N)-**2**

Figure 6. The differing Overhauser enhancements observed at the benzylic protons of [*dl*]-[^{13}C-**2**] and [*meso*]-[^{13}C-**2**] on irradiation of the ^{12}C methyl group ([D$_8$]toluene, −30°C, 500 MHz).

Almost equal Overhauser enhancements were observed at the diastereotopic benzylic signals (1.7 versus 1.3%) in the minor isomer whilst in the major isomer, the NOE with one of the diastereotopic benzylic proton signals was enhanced by a factor of 1.6 over that with the other (3.7 versus 2.3%). These results may be explained by the major isomer being the [*dl*]-[^{13}C-**2**] form in which both methyl groups have two neighbouring benzyl groups and the minor isomer being the [*meso*]-[^{13}C-**2**] form in which each methyl group has only one. Similar effects were observed with the protonated form (i.e. [^{13}C-**2**H]$^+$[I]$^-$) and this then supports the assignment of the structure of the major isomer of the free base in solution as being [*dl*]-[**2**].

Stereodynamics of 2 − Effect of Solvent Polarity

In contrast to [**2**H]$^+$[I]$^-$,[11] the rate of interconversion of [*dl*]- and [*meso*]-[**2**] is fast enough to allow rate constants to be determined by NMR line-shape analysis. The ^{1}H NMR of **2** as a ca. 0.08 M solution in [D$_8$]toluene, was recorded at various temperatures between −80 and +100°C. At the low temperature limit, sharp signals assignable as those from [*dl*]-[**2**] and [*meso*]-[**2**] (vide supra) were evident. On warming, both the benzylic and the methyl signals of the two isomers broadened and coalesced. Above the high-temperature limit (100°C) a single set of sharp resonances corresponding to the time-averaged spectrum of the two diastereomers was observed. Analysis of the series of spectra is complicated by the following two features. Firstly, the population of the two diastereomers is unequal, thus the coalescence temperatures cannot be used directly. Secondly, nitrogen inversion-rotation at one centre results in [*dl*]-[**2**] and [*meso*]-[**2**] interconversion (epimerisation) whilst inversion-rotation at both centres results in [*d*]-[**2**] to [*l*]-[**2**] interconversion or vice versa. (automerisation, topomerisation[16]). Both epimerisation and topomerisation result in line-broadening due to exchange (diastereotopic or chemical) in the benzylic resonances and thus only the methyl resonances allow selective study of [*dl*]-[**2**] and [*meso*]-[**2**] interconversion. However, the chemical shift difference of the methyl groups in the slow exchange regime is low (Δδ, −45°C, ca. 4 Hz) and thus analysis of line shape inaccurate.[17]

We therefore turned to analysis of the variable temperature ^{13}C{^{1}H} NMR spectrum of [^{13}C-**2**]. Here, analysis of the line-shape of the well dispersed methyl group singlets (Δδ, −31°C, ca. 230 Hz) allows the rate of {[*meso*]<−>[*dl*]} interconversion to be calculated without the automerisation process {[*d*]<−>[*l*]} interfering.

Using a series of spectra obtained in the slow exchange regime (−50 to + 20°C) the effect of temperature on the equilibrium population was analysed in the form of a van′t Hoff plot (ln$K$ versus 1/T) from which the ground state energy differences (ΔG°) between [*dl*]-[^{13}C-**2**] and [*meso*]-[^{13}C-**2**], together with enthalpic (ΔH°) and entropic (ΔS°) parameters are readily obtained − Table 1.

Table 1. Thermodynamic differences (and estimated errors) between ground state [*meso*]-[^{13}C-**2**] and [*dl*]-[^{13}C-**2**] in [D$_7$]DMF, [D$_8$]toluene, [D$_6$]acetone and [D$_2$]-1,1,2,2-tetrachloroethane. Parameters extracted by linear regression of a van′t Hoff type analysis of ^{13}C-NMR data between −50 and +10°C.

Solvent	ε[a]	$\Delta H°_{dl\text{-}meso}$[b] kcal mol^{-1}	$\Delta S°_{dl\text{-}meso}$[b] cal K^{-1}mol^{-1}	$\Delta G^{298}{}_{dl\text{-}meso}$[b] kcal mol^{-1}
[D$_7$]DMF	38.3	−0.64 (± 0.03)	−0.18 (± 0.13)	−0.58 (± 0.07)
[D$_6$]acetone	20.7	−0.64 (± 0.02)	+ 0.14 (± 0.06)	−0.68 (± 0.04)
[D$_2$]TCE[c][d]	8.5	−0.74 (± 0.02)	−0.47 (± 0.07)	−0.60 (± 0.05)
[D$_8$]toluene	2.4	−0.71 (± 0.02)	−0.11 (± 0.08)	−0.68 (± 0.04)

[a] Solvent dielectric constant at 298 K. − [b] $\Delta X° = (X°_{dl}) - (X°_{meso})$; X = H, S, or G. − [c] [D$_2$]TCE = 1,2-[^{2}H$_2$]-1,1,2,2-tetrachloroethane. − [d] m.p. [D$_2$]TCE = −44°C, data obtained between −40 and 0°C.

The predicted population and chemical shift difference (Δδ versus T) were then extrapolated into the intermediate and fast exchange regime where iterative full band-shape simulation allowed extraction of rates of exchange. Identical experiments were performed in [D$_7$]DMF, [D$_2$]1,1,2,2-tetrachloroethane (Figure 7) and [D$_6$]acetone.

Calculated rate constants are given in Table 2 and thermodynamic parameters extracted by Eyring-type analysis in Table 3.

Representative Eyring analyses for the rates of interconversion of [*dl*]- and [*meso*]-isomers of [^{13}C-**2**] in [D$_7$]DMF and in [D$_8$]toluene are given in Figure 8.

Most notable are the effect of solvent on the entropic ($T\Delta S^{\neq}$) and enthalpic ($\Delta H^{\neq}$) contributions to the transition

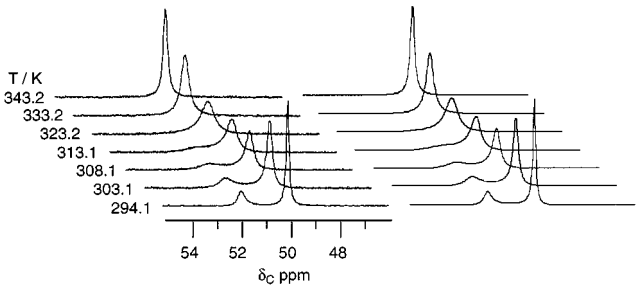

Figure 7. Full band-shape analysis obtained by iterative fitting of simulated spectrum (right hand series) to observed spectrum (left hand series) for the methyl singlets in the ^{13}C NMR (100 MHz) sub-spectrum of [*dl*]-[^{13}C-**2**] and [*meso*]-[^{13}C-**2**] in [D_2]-1,1,2,2-tetrachloroethane

state barrier. Since ground state energy differences are small, these are approximately equal in either direction − Table 3.

Such large entropy changes are not solely due to unimolecular effects such as increasing rigidity and lowered degrees of freedom and clearly the more polar or polarisable the solvent the more ordered it is about the transition state relative to the ground state. The effect may be explained in a qualitative manner by consideration of the lone pair vectors in ground state [*dl*]-**2** and [*meso*]-**2** and how these will change on approach to the transition state.

In the ground state the two lone pair vectors are opposed in both [*dl*]-**2** and [*meso*]-**2**. In [*dl*]-**2** the disposition of the benzyl and methyl groups is symmetrical and there is essentially no net orthogonal dipole. Although in [*meso*]-**2** the inequivalent positioning of both the benzyl and the methyl groups (in a similar manner to [**6***endo*] and [**6***exo*]) means that the molecule is chiral, the barrier to automerisation[18] is expected to be low[19] and thus there should be no net time-average dipole. The ground state energy difference between [*dl*]-**2** and [*meso*]-**2** is low (at 298 K, ca. 0.6−0.7 kcal·mol^{-1}) and the effect of solvent on this small energy difference is not open to simple interpretation.

On approach to the transition state, the nitrogen centre undergoing correlated rotation-inversion is trigonalised and thus the remaining tetrahedral nitrogen centre causes a

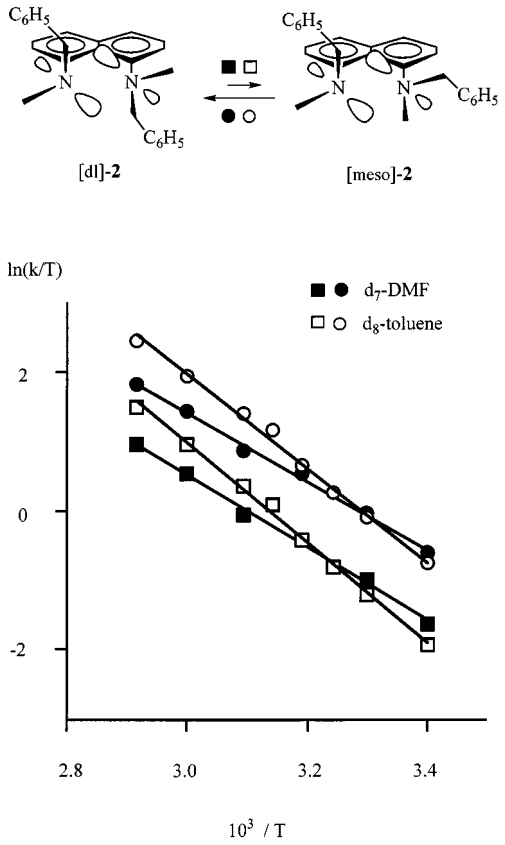

Figure 8. Eyring analysis of rates of interconversion in [D_7]DMF (filled symbol) and [D_8]toluene (open symbol) of [*dl*] to [*meso*] (squares) and [*meso*] to [*dl*] (circles) diastereomers of **2**; data obtained by ^{13}C-NMR full band-shape analysis

moderate net dipole (relative to the ground state). The surrounding solvent will order itself such that its own dipole opposes the transition state dipole. At lower temperatures the polar solvent is able to increase the rate, relative to a less polarisable solvent, through solvation and reduction of the net transition state dipole in the solvent shell. However, at increasing temperatures, the increasing energetic cost of solvent order ($T\Delta S^{\neq}$) eventually results in greater rates in the less polarisable solvents. The loss of entropy of mixing

Table 2. First-order rate constants (with estimated errors) for the interconversion of [*dl*]-[^{13}C-**2**] and [*meso*]-[^{13}C-**2**] in [D_7]DMF, [D_6]acetone, [D_2]-1,1,2,2-tetrachloroethane, and [D_8]toluene at various temperatures as determined by ^{13}C-NMR full band-shape analysis of the ^{13}C-labelled methyl groups.

T [K]	[D_7]DMF[a]		[D_6]acetone[b]		[D_8]toluene[c]		[D_2]TCE[d][e]	
	$k_{dl\text{-}meso}$ (error ±)	$k_{meso\text{-}dl}$ (error ±)	$k_{dl\text{-}meso}$ (error ±)	$k_{meso\text{-}dl}$ (error ±)	$k_{dl\text{-}meso}$ (error ±)	$k_{meso\text{-}dl}$ (error ±)	$k_{dl\text{-}meso}$ (error ±)	$k_{meso\text{-}dl}$ (error ±)
293.7	58(3)	158(9)	53(2)	169(6)	43(3)	136(8)	41(1)	115(4)
299.0	−[f]	−[f]	74(3)	231(8)	−[f]	−[f]	−[f]	−[f]
303.2	111(4)	294(11)	105(3)	322(7)	89(7)	272(19)	79(3)	215(7)
307.9	−[e]	−[e]	154(5)	467(16)	135(2)	403(4)	115(5)	306(17)
312.9	204(7)	525(18)	231(13)	688(40)	201(11)	590(31)	168(8)	442(18)
318.1	−[e]	−[e]	335(13)	982(40)	346(18)	997(51)	−[e]	−[e]
323.1	301(14)	754 (35)	440(11)	1270(31)	456(11)	1290(31)	365(9)	925(22)
333.2	566(11)	1386(27)	−[f]	−[f]	853(6)	2336(15)	710(7)	1738(17)
343.3	884(13)	2119(31)	−[f]	−[f]	1515(27)	4015(74)	1252(9)	2971(21)

[a] $\ln K_{eq} = ([dl]_{eq}/[meso]_{eq}) = (321/T) - 0.09$; $\Delta\delta$ (Hz) = 387.75 − 0.607 *T*. − [b] ln*K*eq = (320/*T*) + 0.07; $\Delta\delta$ (Hz) = 378.6 − 0.525 *T*. − [c] ln*K*eq = (355/*T*) − 0.06; $\Delta\delta$ (Hz) = 328.9 − 0.42 *T*. − [d] [D_2]TCE = 1,2-[$^2H_2$]-1,1,2,2-tetrachloroethane. − [e] ln*K*eq = (370/*T*) − 0.238; $\Delta\delta$ (Hz) = 231.6 − 0.150 *T*. − [f] Not determined.

of enantiomers [S_{mix} = R(ln 2)] and the gain in entropy by desymmetrisation [S_{sym} = −R(ln 2)] that [*dl*]-**2** experiences on approach to the transition state should cancel. Schematic representations of ground and transition state dipoles and activation energies are shown in Figure 9.

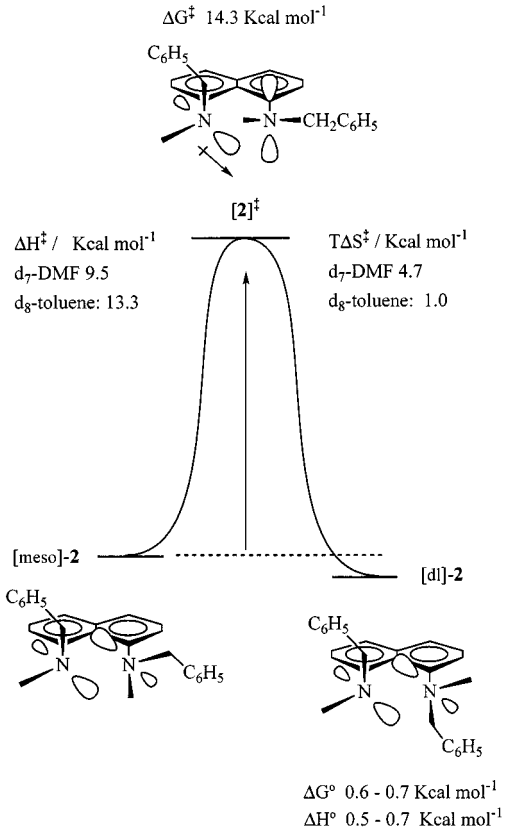

Figure 9. Schematic representation of the thermodynamics for interconversion of [*dl*]-[^{13}C-**2**] and [*meso*]-[^{13}C-**2**], in [D_7]DMF versus [D_8]toluene at 298 K, emphasising the dipole generation on approach to [**2**]$^+$. Data is for approach to transition state from [*meso*]-[^{13}C-**2**] ground state and are taken from Tables 1 and 3.

As a crude measure of dipole stabilising ability, the dielectric constant of the undeuterated solvents (DMF, acetone, tetrachloroethane, and toluene) can be employed. These values correlate very approximately with both the enthalpy and entropy of activation and this serves to support the interpretation of dipole development as being the cause of the solvent effect.

Conclusions

An equilibrium mixture of [*dl*]-[**2**H]$^+$[I]$^-$ and [*meso*]-[**2**H]$^+$[I]$^-$ is formed, with a pseudo zero-order rate dependence, on dissolution of diamine **6** in methyliodide (or diamine **7** in benzyliodide). Deprotonation by aqueous hydroxide affords the *N,N′*-chiral proton sponge **2**, initially as the sesquihydrate, in good yield. The stereostructures of **2** and [**2**H]$^+$ in solution were elucidated by ^{1}H-NMR NOE utilising a ^{13}C label to effect isotopic desymmetrisation. The solid state structure of the major [*dl*]-**2** form was determined by single crystal X-ray diffraction and shows, as expected, substantial distortion of the naphthalene ring through steric and stereoelectronic effects. Also as expected, this strain is not present in the protonated form [*dl*]-[**2**H]$^+$[I]$^-$ as was evidenced by earlier X-ray crystallography.[8] The stereodynamics of **2** was studied by full band-shape analysis of variable temperature ^{1}H and ^{13}C NMR. At ambient temperature, the major isomer [*dl*]-**2** is slightly more favoured in toluene than it is in DMF. Approach to the transition state for interconversion of [*dl*]-**2** and [*meso*]-**2** results in a net dipole and, consequently, the greater the dielectric constant of the solvent, the greater the net decrease in entropy on approach to the transition state. The activation barriers to interconversion of [*dl*]-**2** and [*meso*]-**2** (ca. 15 kcal·mol^{-1} at −5°C) may be compared with that determined by Alder and Anderson[19] for the automerisation of **8** (ca. 13 kcal·mol^{-1} at −5°C, based on ^{1}H-NMR coalescence of the diastereotopic benzylic resonances). The small increase (ca. 2 kcal mol^{-1}) supports the notion that passage of the methyl group through the intra-nitrogen gap is the more favoured process for rotation-inversion which may well be correlated (synchronous).

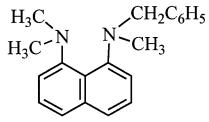

8

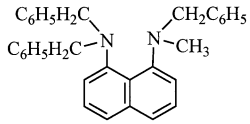

9

Future work will concentrate on further elucidating the difference between benzyl and methyl groups in these systems (by further study of **8** and **9**) and also on the effect of substitution at the 2-,4-,5-, and 7- positions of the naphthalene ring which may exert substantial steric and electronic

Table 3. Thermodynamic parameters (298 K) for interconversion of [*dl*]-[^{13}C-**2**] and [*meso*]-[^{13}C-**2**] in [D_7]DMF, [D_6]acetone, [D_2]-1,1,2,2-tetrachloroethane and [D_8]toluene. Parameters extracted by linear regression of an error-weighted Eyring type analysis of data from Table 2

Solvent	dielectric constant ε	$\Delta H^{\neq}_{dl}$ kcal mol^{-1}	$\Delta S^{\neq}_{dl}{}^{-1}$ cal K^{-1}mol^{-1}	$\Delta G^{\neq}_{dl}$ kcal mol^{-1}	$\Delta H^{\neq}_{meso}$ kcal mol^{-1}	$\Delta S^{\neq}_{meso}$ cal K^{-1}mol^{-1}	$\Delta G^{\neq}_{meso}$ kcal mol^{-1}
[D_7]DMF	38.3	10.0 (± 0.2)	−16.0 (± 0.7)	14.8 (± 0.4)	9.5 (± 0.2)	−15.8 (± 0.7)	14.2 (± 0.4)
[D_6]acetone	20.7	13.4 (± 0.2)	−5.3 (± 0.9)	15.0 (± 0.5)	12.7 (± 0.2)	−5.0 (± 0.6)	14.2 (± 0.4)
[D_2]TCE[a]	8.5	13.3 (± 0.2)	−6.0 (± 0.5)	15.0 (± 0.3)	12.6 (± 0.2)	−6.3 (± 0.6)	14.4 (± 0.4)
[D_8]toluene	2.4	14.0 (± 0.2)	−3.4 (± 0.7)	15.0 (± 0.4)	13.3 (± 0.2)	−3.5 (± 0.7)	14.3 (± 0.5)

[a] [D_2]TCE = 1,2-[$^2H_2$]-1,1,2,2-tetrachloroethane.

influence on the rotation-inversion barrier. If the barrier can be raised sufficiently (by approximately 15 kcal·mol^{-1}) then compounds analogous to **2** may become useful for absolute or relative stereochemical control in organic synthesis.

Experimental Section

General: All manipulations and reactions were carried out under N_2 or Ar using standard Schlenk techniques, with the exception of the acid hydrolyses. − NMR experiments were performed on JEOL Lambda 300, JEOL GX400, and JEOL Alpha 500 instruments. − Mass spectra were obtained using both CI and EI sources on a Fisons *Micromass Autospec* mass spectrometer. − Elemental analysis of the compounds were performed by the analytical service of the School of Chemistry, University of Bristol. − Column and thin layer chromatography was performed on activated neutral alumina ca. 150 mesh and, when necessary, column chromatography was performed with nitrogen or argon saturated solvents. − All solvents used for reactions were anhydrous. 9-BBN, MeI, CD_3I and $^{13}CH_3$, benzylchloride, and benzylbromide were purchased from Aldrich and used as received. 1,8-diaminonaphthalene (Aldrich) was purified by either Soxhlet extraction using pentane or by distillation (ca. 144°C, 0.9 Torr).

X-ray Crystallography: X-ray measurements were made using a Bruker SMART CCD area-detector diffractometer with Mo-K_α radiation (λ = 0.71073 Å). Crystallographic data (excluding structure factors) for the structure of **2** has been deposited with the Cambridge Crystallographic Data Centre as supplementary publication no. CCDC-116496. Copies of the data can be obtained free of charge on application to CCDC, 12 Union Road, Cambridge CB2 1EZ, UK (Fax: +44-1223/336-033; E-mail: deposit@ccdc.cam.ac.uk).

Synthesis of Compounds

***N*-(9-[3.3.0]Borabicyclononyl)-1,8-diaminonaphthalene (3):** This was prepared by following the procedure of Kol et al.[12] Thus, a 0.25 M solution of (9-BBN)$_2$ (2.008 g, 8.23 mmol) in freshly distilled hexane (35 mL) was added to a solution of 1,8-diaminonaphthalene (2.603 g, 16.45 mmol) in ether (40 mL). The resulting bright yellow coloured solution was stirred rapidly to maximise hydrogen evolution, which continued for approximately one hour. After a further 12 hours a yellow precipitate had formed. The ether was removed via cannula and the solid was washed with ether (10 mL). The resulting yellow solid was dried in vacuo to afford the title compound (4.174 g, 91.2%). − $C_{18}H_{23}BN_2$ (278.24) calcd. C 77.70, H 8.35, N 10.07, found C 77.81, H 8.48, N 10.28%.

***N,N′*-Bis(benzyl)-1,8-diaminonaphthalene (4):** *t*BuOK (1.753 g, 15.6 mmol) was added to a solution of **3** (2.174 g, 7.8 mmol) in THF (70 mL). The solution was stirred at room temperature for 30 minutes after which time it was dark brown in colour. Benzylbromide (0.93 mL, 1.337 g, 7.8 mmol) was added to the solution, resulting in a slightly exothermic reaction. The solution was left stirring at room temperature for 10 minutes after which a further portion of benzylbromide (0.93 mL, 1.337 g, 7.8 mmol) was added resulting in a slightly exothermic reaction. The solution was left stirring overnight at room temperature. 1 M HCl (150 mL) was added and the resultant solution stirred at room temperature for two days. After neutralisation with 3 M NaOH (ca. 5 mL) the resultant bright yellow solution was extracted with dichloromethane (100 mL), dried ($MgSO_4$), and the solvent removed in vacuo to afford an orange crystalline solid. Purification by chromatography on alumina eluting with 19:1 hexane/EtOAc gave the title compound as a white solid (2.376 g, 90%). m.p. 97−105°C (darkens at 93°C). MS (CI): *m/z* (%) 339 (100), 338 (92), 247 (40), 230 (10), 169 (12), 115 (6), 91 (20). HRMS (CI) $C_{24}H_{23}N_2$ requires *m/z* 339.186124, found 339.185196. − ^{1}H NMR (C_6D_6, 300 MHz, 21°C, TMS) 3.92 (br. s, 4 H; 2 × CH_2), 5.64 (br. s, 2 H; 2 × NH), 6.48 [dd, ^3J(H,H) = 7.5, ^4J(H,H) = 1.1, 2 H; 2 × C(2)-H], 6.96-7.01 (m, 6 H; 2 × *p*-Ph, 4 × *m*-Ph), 7.02−7.09 (m, 4 H; 2 × *o*-Ph), 7.24 [dd, ^3J(H,H) = 7.5, 8.2, 1 H; 2 × C(3)-H], 7.36 [dd, ^3J(H,H) = 8.2, ^4J(H,H) = 1.1, 2 H; 2 × C(4)-H].

***N*-(Benzyl)-*N′*-(benzylmethyl)-1,8-diaminonaphthalene (6):** 1,8-bis(benzylamino)naphthalene **4** (514 mg, 1.52 mmol) was dissolved in THF (15 mL) and the resulting light brown solution added via cannula to NaH (73 mg, 3.04 mmol) resulting in vigorous hydrogen evolution. The solution was stirred at room temperature for 30 minutes, after which methyliodide (0.19 mL, 435 mg, 3.04 mmol) was added. After heating to reflux for 1 hour, the now paler solution was cooled to room temperature and 3 M NaOH (30 mL) added. The product was extracted with degassed, nitrogen saturated ether (25 mL) and the orange organic phase filtered through a pad of alumina. The solvent was removed in vacuo to give a viscous dark orange oil which was purified by chromatography on alumina eluting with 39:1 hexane/EtOAc to afford the title compound as a pale brown oil (470 mg, 87.5%). Over a period of a few weeks the oil crystallised to give a white solid, m.p. 69−74°C; $C_{25}H_{24}N_6$ (352.51) calcd. C 85.19, H 6.86, N 7.95; found C 85.17, H 7.50, N 7.64%. − IR (Oil) $\tilde{\nu}$ = 3240 (N−H), 3059, 3027, 2958, 2850, 1694, 1600, 1494, 1396, 1294, 1028, 816, 760, 744, 698 cm^{-1}. − ^{1}H NMR (C_6D_6, 300 MHz, 21°C, TMS) 2.33 (s, 3 H; CH_3), 3.63 [d, ^2J(H,H) = 12.9, 1 H; CH_BHPh], 4.01 [d, ^2J(H,H) = 12.9, 1 H; CHH_APh], 4.3 (second order m, 2 H; PhCH_2NH), 6.52 [dd, ^3J(H,H) = 7.7, ^4J(H,H) = 1.1, 1 H; C(7)-H], 6.89 [dd, ^3J(H,H) = 7.4, ^4J(H,H) = 1.1, 1 H; C(2)-H], 6.93−7.01 (m, 5 H; Ph) 7.05−7.15 (m, 3 H; *m*-BnNH, *p*-BnNH), 7.15−7.23 [m, 2 H; C(3)-H, C(5)-H], 7.25−7.30 (m, 2 H; *o*-BnNH), 7.30 [dd, ^3J(H,H) = 7.7, 7.7, 1 H; C(6)-H], 7.55 [dd, ^3J(H,H) = 8.1, ^4J(H,H) = 0.9, 1 H; C(4)-H], 9.74 [t, ^3J(H,H) = 4.9, 1 H; NH]. − ^{13}C{^{1}H} NMR (C_6D_6, 75 MHz, 21°C, C_6D_6) 44.3 (CH_3), 48.8 [C(1′′)-*C*H_2NH], 62.5 [C(1′)-*C*H_2NCH$_3$], 104.8 [C(7)], 116.7 [C(5)], 117.9 [C(2)], 125.8 [C(3)], 127.1 [C(4)], 2 × 127.6 [C(4′), C(6)], 127.8 [C(2′′)], 128.0 [C(4′′)], 128.2 [C(3′′)], 128.5 [C(3′)], 129.3 [C(2′)], 130.0 [C(9)], 138.2 [C(1′), C(1′′)], 140.7 [C(8)], 147.8 [C(10)], 152.1 [C(1)]. − MS (EI): *m/z* (%) 352 (58) [M$^+$], 337 (10) [M$^+$ − Me], 273 (8), 261 (26) [M$^+$ − Bn], 244 (26) [M$^+$ − BnMe], 230 (16), 183 (22), 170 (100) [M$^+$ − Bn$_2$], 154 (14) [M$^+$ − Bn$_2$Me]. HRMS (EI) $C_{25}H_{24}N_2$ requires: 352.193949, found: 352.192627.

^{13}C-**6** was prepared in similar yields, by identical procedure using 91.4% and > 99% ^{13}C-MeI. − ^{1}H NMR (C_6D_6, 300 MHz, 21°C, TMS) 2.33 [d, ^1J(H,C) = 135.5, 3 H; $^{13}CH_3$], 3.64 [dd, ^2J(H,H) = 13.0, ^3J(H,C) = 4.2, 1 H; CH_BHPh], 4.01 [dd, ^2J(H,H) = 13.0, ^3J(H,C) = 5.7, 1 H; CHH_APh], 4.31 (second order m, 2 H; PhCH_2NH) 6.54 [dd, ^3J(H,H) = 7.7, ^4J(H,H) = 1.0, 1 H; C(7)-H], 6.89 [dd, ^3J(H,H) = 7.5, ^4J(H,H) = 1.1, 1 H; C(2)-H], 6.93−7.01 (m, 5 H; Ph), 7.05−7.15 (m, 3 H; *m*-BnNH, *p*-BnNH), 7.15−7.23 [m, 2 H; C(3)-H, C(5)-H], 7.25−7.30 (m, 2 H; *o*-BnNH), 7.30 [dd, ^3J(H,H) = 7.7, 7.7, 1 H; C(6)-H], 7.55 [dd, ^3J(H,H) = 8.1, ^4J(H,H) = 0.9, 1 H; C(4)-H], 9.74 [t, ^3J(H,H) = 4.9, 1 H; NH].

Hydrogen Iodide Salt of *N,N′*-Bis(benzylmethyl)-1,8-diaminonaphthalene ([2H]$^+$[I]$^-$): *N*-(benzyl)-*N′*-(benzylmethyl)-1,8-diaminonaphthalene **6** (0.313 g, 0.885 mmol) was dissolved in methyliodide (1.87 mL, 30.1 mmol) in an ampoule resulting in an dark orange

solution. The ampoule was sealed and the solution was left a room temperature for two days during which crystallisation occurred at the upper surface of the solution. The excess methyliodide was decanted. The pale yellow crystals were washed with a small amount of methyliodide (ca. 0.5 mL) and the washings were added to the mother liquors. The remaining pale yellow solid was washed with ether (ca. 1 mL) and dried in vacuo to give pale yellow crystals. The crystalline solid was dissolved in a minimum volume of CH_2Cl_2 and layered carefully with 5 times the volume of ether. The solution was left until diffusion of the two layers was complete, after which time the solvent was decanted and the solid dried in vacuo to give the title compound as a pale yellow solid. A second crop of [**2**H]$^+$[I]$^-$ was obtained from the methyliodide mother liquors and washings after a period of a further two days. In total [**2**H]$^+$[I]$^-$ (372 mg, 85%). m.p. 171−175°C, $C_{26}H_{27}N_2I$ (494.45) calcd. C 63.20, H 5.50, N 5.70, found C 63.14, H 5.58, N 5.78%. − IR (KBr) $\tilde{\nu}$ = 3011 b (N−H stretch), 2366 w, 1450 s, 1372 m, 1222 m, 1150 m, 1011 m, 905 w, 833 s, 772 s, 750 s, 700 s cm^{-1}. − ^{1}H NMR (CD_2Cl_2, 300 MHz, 21°C, TMS) [*dl*]-[**2**H]$^+$[I]$^-$: 3.14 [d, ^3J(H,H) = 2.6, 6 H; 2 × CH_3], 4.65 [dd, ^2J(H,H) = 12.7, ^3J(H,H) = 1.1, 2 H; 2 × C*H*HPh], 4.79 [dd, ^2J(H,H) = 12.6, ^3J(H,H) = 1.6, 2 H; 2 × CH*H*Ph], 7.06 (m, 4 H; 2 × *o*-Bn) 7.13 (m, 4 H; 2 × *m*-Bn), 7.20−7.35 (m, 2 H; 2 × *p*-Bn), 7.54 [dd, ^3J(H,H) = 7.5, ^4J(H,H) = 1.7, 2 H; C(2)-H, C(7)-H], 7.58 [dd, ^3J(H,H) = 7.5, 7.5, 2 H; C(3)-H, C(6)-H], 7.96 [dd, ^3J(H,H) = 7.5, ^4J(H,H) = 1.7, 2 H; C(4)-H, C(5)-H], 18.1 (br. s, 1 H; NH); [*meso*]-[**2**H]$^+$[I]$^-$; 3.37 ^3J[H,H) = 2.7, 6 H; 2 × CH_3], 4.27 [dd, ^2J(H,H) = 13.2, ^3J(H,H) = 1.5, 2 H; 2 × C*H*HPh], 4.74 [dd, ^2J(H,H) = 13.2, ^3J(H,H) = 2.9, 2 H; 2 × C*H*HPh], aromatic protons belonging to the *meso* isomer not distinguishable), 17.4 (br. s, 1 H; NH). − ^{13}C{^{1}H} NMR (CD_2Cl_2, 75 MHz, 21°C, CD_2Cl_2) [*dl*]-[**2**H]$^+$[I]$^-$; 44.9 (CMe), 63.1 (CBn), 121.8 [C(1)], 123.2 [C(2)], 126.7 [C(3)], 127.8 (CH*o*-arom), 129.5 (CH*p*-arom), 129.7 [C(4)], 131.6 (C*i*-arom), 131.7 (CH*m*-arom), 135.5 [C(10)], 142.2 [C(9)]; [*meso*]-[**2**H]$^+$[I]$^-$; 46.1 (CMe), 60.6 (CBn), 121.8 [C(1)], 123.9 [C(2)], 126.7 [C(3)], 128.9 (CH*o*-arom), 129.6 (CH*p*-arom), 129.9 [C(4)], 131.6 (C*i*-arom), 132.0 (CH*m*-arom), 135.5 [C(10)], 142.2 [C(9)]. − MS (CI): *m*/*z* (%) 368 (14) [MH$^+$ − HI], 278 (63) [MH$^+$ − BnHI], 187 (10) [MH$^+$ − Bn_2HI], 172 (2) [MH$^+$ − Bn_2MeHI], 157 (2) [MH$^+$ − Bn_2Me_2HI].

^{13}CMe-[**2**H]$^+$[I]$^-$ was obtained in similar yield, by identical procedure using ^{13}C-**6**. − ^{1}H NMR (CD_2Cl_2, 500 MHz, 28°C, TMS) [*dl*]-[^{13}CMe-**2**H]$^+$[I]$^-$; 3.127 [dd, ^1J(H,C) = 140.9, ^3J(H,H) = 2.5, 3 H; $^{13}CH_3$], 3.135 [d, ^3J(H,H) = 2.5, 3 H; $^{12}CH_3$], 4.65 [dd, ^2J(H,H) = 12.5, ^3J(H,H) = 1.1, 2 H; 2 × C*H*HPh], 4.79 [dd, ^2J(H,H) = 12.5, ^3J(H,H) = 1.6, 2 H; 2 × CH*H*Ph], 7.06 (m, 4 H; 2 × *o*-Bn), 7.13 (m, 4 H; 2 × *m*-Bn), 7.20-7.35 (m, 2 H; 2 × *p*-Bn), 7.54 [dd, ^3J(H,H) = 7.5, ^4J(H,H) = 1.7, 2 H; C(2)-H, C(7)-H], 7.58 [dd, ^3J(H,H) = 7.5, 7.5, 2 H; C(3)-H, C(6)-H], 7.96 [dd, ^3J(H,H) = 7.5, ^4J(H,H) = 1.7, 2 H; C(4)-H, C(5)-H], 18.1 (br. s, 1 H; NH).

***N,N′*-Bis(benzylmethyl)-1,8-diaminonaphthalene 2:** An orange solution of [**2**H]$^+$I$^-$ (105 mg, 0.21 mmol) in CH_2Cl_2 (15 mL) was shaken with three portions of 4 M NaOH (ca. 5 mL). The orange organic layer was separated and dried with NaOH granules for approximately 30 seconds after which the solvent was removed in vacuo to give the title compound as an off-white powdery solid (76 mg, 98%). $(C_{26}H_{26}N_2)_2(H_2O)_3$ (787.48) calcd. C 79.35, H 7.43, N 7.12, found C 79.09, H 7.26, N 6.87. m.p. 138−141°C. On cooling, toluene (or acetone) solutions of **2** afforded pale fawn crystals of **2** free of water $C_{26}H_{26}N_2$ (366.5) calcd. C 85.21, H 7.15, N 7.64, found C 85.37, H 7.24, N 7.40. m.p. 142−144°C. − ^{1}H NMR ($C_6D_5CD_3$, 400 MHz, −45°C, TMS) [*dl*] isomer: 2.46 (s, 6 H; 2 × CH_3), 4.02 [d, ^2J(H,H) = 13.5, 2 H; C*H*HPh], 4.24 [d, ^2J(H,H) = 13.5, 2 H; CH*H*Ph], 6.61 [d, ^3J(H,H) = 7.3, 2 H; C(2)-H, C(7)-H], 6.69 (m, 2 H; 2 × *p*-Bn) 6.95-7.10 (m, 8 H; 2 × *o*-Bn, 2 × *m*-Bn), 7.20 [dd, ^3J(H,H) = 8.1, 7.3, 2 H; C(3)-H, C(6)-H], 7.46 [^3J(H,H) = 8.1, 2 H; C(4)-H, C(5)-H]. [*meso*] isomer; 2.42 (s, 6 H; 2 × *meso*-CH_3). both isomers: ^{1}H NMR ($C_6D_5CD_3$, 400 MHz, 70°C, TMS) 2.62 (s, 6 H; 2 × CH_3), 4.22 (s, 4 H; 2 × CH_2Ph), 6.77 [d, ^3J(H,H) = 7.6, 2 H; C(2)-H, C(7)-H], 6.84 (m, 2 H; 2 × *p*-Bn), 7.02−7.04 (m, 8 H; 2 × *o*-Bn, 2 × *m*-Bn), 7.18 [dd, ^3J(H,H) = 7.6, 8.1, 2 H; C(3)-H, C(6)-H], 7.41 [^3J(H,H) = 8.1, 2 H; C(4)-H, C(5)-H]. − ^{13}C{1H} NMR (CD_2Cl_2, 75 MHz, 21°C, CD_2Cl_2) 39.6 (b, CH_3), 61.9 (b, CH_2), 115.1 [C(2,7)], 122.5 [C(4,5)], 125.6 [C(3,6)], 127.0 [2 × C(4′)], 128.2 [4 × C(3′)], 129.1 [b, 4 × C(2′)], 138.4 [2 × C(1′)], 138.5 [C(9)], 150.0 [C(1,8)].

***N,N′*-Bis(methyl)-1,8-diaminonaphthalene 5:** The synthesis of *N,N′*-bis(methyl)-1,8-diaminonaphthalene **5** was performed as described above for *N,N′*-bis(benzyl)-1,8-diaminonaphthalene **4**. Using **3** (917 mg, 3.30 mmol), *t*BuOK (814 mg, 7.26 mmol), and methyliodide (0.45 mL, 1030 mg, 7.26 mmol) to afford the title compound (219 mg, 36%). m.p. 77−80°C (ref.[20] 103−104°C). − ^{1}H NMR (C_6D_6, 300 MHz, 21°C, TMS) 2.54 (s, 6 H; 2 × CH_3), 4.97 (br. s, 2 H; 2 × NH), 6.54 [second order m, 2 H; C(2)-H, C(7)-H], 7.32 [second order m, 2 H; C(3)-H, C(6)-H], 7.35 [second order m, 2 H; C(4)-H, C(5)-H].

***N*-(Methyl)-*N′*-(benzylmethyl)-1,8-diaminonaphthalene 7:** This was prepared as described above for **6** from *N,N′*-bis(methyl)-1,8-diaminonaphthalene **5** (122 mg, 0.655 mmol), NaH (32 mg, 1.310 mmol), and benzyliodide (0.166 mL, 286 mg, 1.310 mmol) to give the title compound as a viscous yellow oil (78 mg, 43%). − IR (Oil) $\tilde{\nu}$ = 3253, 2924, 1701, 1580, 1536, 1495, 1453, 1071, 1026, 761, 742, 699. cm^{-1}. − ^{1}H NMR (C_6D_6, 300 MHz, 21°C, TMS) 2.01 (s, 3 H; CH_3NBn), 2.44 [d, ^3J(H,H) = 5.1, 3 H; CH_3NH], 3.27 [d, ^2J(H,H) = 12.8, 1 H; C*H*HPh], 3.71 [d, ^2J(H,H) = 12.8, 1 H; CH*H*Ph], 6.18 [d, ^3J(H,H) = 7.5, 1 H; C(7)-H], 6.55 [dd, ^3J(H,H) = 7.4, ^4J(H,H) = 1.1, 1 H; C(2)-H], 6.65−6.84 (m, 5 H; Ph), 6.90 [m, 1 H; C(3)-H], 6.95 [m, 1 H; C(5)-H], 7.13 [dd, ^3J(H,H) = 7.5, ^4J(H,H) = 1.0, 1 H; C(6)-H], 7.26 [dd, ^3J(H,H) = 9.0, ^4J(H,H) = 0.9, 1 H; C(4)-H], 8.99 (m, 1 H; NH). − ^{13}C NMR (C_6D_6, 75 MHz, 21°C, C_6D_6) 30.3, 32.4, 43.3, 62.4, 103.3, 115.9, 117.3, 125.5, 126.6, 126.7, 127.8, 128.2, 128.6, 128.7, 129.6, 130.4, 131.1. − MS (CI): *m*/*z* (%) 277 (84) [MH$^+$], 262 (2) [MH$^+$ − Me], 186 (21) [MH$^+$ − Bn], 171 (5) [MH$^+$ − BnMe], 156 (4) [M$^+$ − $BnMe_2$], 133 (6), 119 (11), 105 (8), 91 (47). HRMS (CI) $C_{19}H_{21}N_2$ requires: 277.17047, found: 277.17086.

Benzyliodide: Benzyliodide was prepared according to the method of Coleman and Hauser.[21] Benzylchloride (6.30 g, 49.8 mmol) was added to a colourless solution of NaI (10.0 g, 66.7 mmol) in acetone (50 mL) resulting in a bright yellow solution and a white precipitate. After 75 min. reflux, the reaction mixture was cooled to room temperature and added to water (100 mL). The orange organic layer was separated, cooled in an ice salt bath and the resulting bright yellow solid recrystallised from EtOH (ca. 3 mL) 5 times giving the title compound as a pale yellow crystalline solid (5.66 g, 52%). m.p. ca. 22°C. − ^{1}H NMR (CH_2Cl_2, 300 MHz, 21°C, TMS) 4.45 (s, 2 H; $PhCH_2$), 7.20−7.32 (m, 3 H; *m*-Ph, *p*-Ph), 7.36−7.41 (m, 2 H; *o*-Ph).

Dynamic NMR: ^{13}C NMR spectra were acquired on a JEOL GX400 instrument fitted with a variable temperature probe. Temperatures were measured by a thermocouple (located within the probe head) which was calibrated by use of a "methanol thermometer"[22] − a technique which employs the temperature-dependent ^{1}H-NMR shift of the hydroxyl proton versus the methyl protons of methanol. The correlation was found to be [$T_{methanol}$ =

$1.0101(T_{thermocouple}) - 3.3463$]. The values measured during the dynamic NMR experiments (293−343 K) were corrected accordingly and are estimated to be accurate to ±0.6 K. Raw FID data (512 scans) was exported (via *g-CVT*) to the commercial software package *g-SPG* where it was processed (16384 points, *without any form of FID weighting*). A window of approximately 900 Hz (containing both $^{13}CH_3$ peaks) was then transferred to *g-NMR* and iteratively compared with simulated spectra (generated with natural line width 0.35 Hz, chemical shift difference predicted by extrapolation, population predicted by van't Hoff analysis and solely the rate of interconversion as a variable) until a satisfactory fit was obtained. Errors for the simulations were then estimated by manually increasing and decreasing the rate of interconversion until the fit became visibly unsatisfactory. By using the errors estimated in both the line-shape analysis and temperature measurement, $\ln(k_{max}/T_{min})$ and $\ln(k_{min}/T_{max})$ were used to calculate errors in data points for the Eyring analyses. The data were weighted by error in the linear regression analysis to provide confidence limits in the entropic and enthalpic contributions to the overall free energy.

Acknowledgments

G. C. L.-J. thanks the Zeneca Strategic Research Fund and Pfizer Ltd. (particularly Dr. Paul Hodgson) for generous donations and the Nuffield Foundation for a start-up grant (SCI/180/96/142). R.L.W. thanks Pfizer Ltd. for a vacation bursary (1998) and for continued support in the form of a CASE award in collaboration with Dr. Paul Hodgson. We thank Professor Gary R. Weisman (University of New Hampshire, USA) for performing some of the initial dynamic NMR simulations. Both he and Professor Roger W. Alder (Bristol) were most encouraging and informative in discussions regarding structures and stereodynamics. Dr. Moshe Kol (Tel Aviv) kindly provided detailed information regarding the preparation and reactions of **3**.

[1] W. G. Brown, N. J. Letang, *J. Am. Chem. Soc.* **1941**, *63*, 358−361.
[2] R. W. Alder, P. S. Bowman, W. R. S. Steele, D. R. Winterman, *J. Chem. Soc., Chem. Commun.* **1968**, 723−724.
[3] Review: H. A. Staab, T. Saupe, *Angew. Chem.* **1988**, *100*, 895; *Angew. Chem. Int. Ed. Engl.* **1988**, *27*, 865−879.
[4] H. A. Staab, C. Krieger, G. Hieber, K. Oberdorf, *Angew. Chem., Int. Ed. Engl.* **1997**, *36*, 1884−1886.
[5] R. W. Alder, N. C. Goode, N. Miller, F. Hibbert, K. P. P. Hunte, H. J. Robbins, *J. Chem. Soc., Chem. Commun.* **1978**, 89−90.
[6] F. Hibbert, S. Phillips, *J. Chem. Research (S)* **1990**, 90−91 and references therein.
[7] Review: A. F. Pozharskii, *Russ. Chem Rev.* **1998**, *67*, 1−24.
[8] Part of this work has appeared in communication form: J. P. H. Charmant, G. C. Lloyd-Jones, T. M. Peakman, R. L. Woodward, *Tetrahedron Lett.* **1998**, *39*, 4733−4736.
[9] The hydrogen bond is weaker than anticipated and thus $[\mathbf{2}H]^+$ is stereolabile at ambient temperature − see references [8] and [11].
[10] For contrasting values of the strength of the hydrogen bond in $[\mathbf{1}H]^+$ see: J. A. Gerlt, M. M. Kreevoy, W. W Cleland, P. A. Frey, *Chemistry &AMPp̄ Biology* **1997**, *4*, 259−267; J. P. Guthrie, *Chemistry & Biology* **1996**, *3*, 163−170; G. H. Barnett, F. Hibbert, *J. Am. Chem. Soc.* **1984**, *106*, 2080; For leading references on asymmetric H-bonds, see: C. L. Perrin, J. B. Nielson, *J. Am. Chem. Soc.* **1997**, *119*, 12734−12741.
[11] We will report on the hydrogen bonding and stereodynamics of $[\mathbf{2}H]^+[I]^-$, in full, elsewhere: G. C. Lloyd-Jones, P. Hodgson, M. Murray, T. M. Peakman, R. L. Woodward, *Chem. Eur. J.,* manuscript in preparation.
[12] G. Bar-Haim, R. Shach, M. Kol, *Chem. Commun.* **1997**, 229−230; G. Bar-Haim, M. Kol, *J. Org. Chem.* **1997**, *62*, 6682−6683.
[13] Under these anionic conditions, the use of a more reactive alkylating agent, e.g. R_2SO_4, is probably required to effect the second alkylation. The NaH/dialkyl sulphate method has been used extensively. Selective trialkylation of 1,8-diaminonaphathalenes with alkyl iodides has also been reported by Pozharskii et al. − see reference [7].
[14] We attempted to estimate the p*K*a of **2** by ^{1}H-NMR measurement of the equilibrium proton distribution after mixing equimolar quantities of $\mathbf{2}H^+$ and **1**. However, the measurement was complicated by a side reaction that resulted in extensive debenzylation. This reaction will be reported, in full, eleswhere.
[15] The assignment was subsequently confirmed by low temperature dissolution − see reference [11].
[16] E. L. Eliel., S. H. Wilen, L. N. Mander, *The Stereochemistry of Organic Compounds*, John Wiley and Sons, Chichester, UK, **1994**.
[17] For a dicussion of systematic errors and inaccuracies in DNMR see, for example, H. Günther, in *NMR spectroscopy*, Second edition, John Wiley and Sons, Chichester, UK, **1995**; J. Sandström, *Dynamic NMR Spectroscopy*, Academic Press, London, **1982**.
[18] In effect it must interconvert object and mirror image, a so-called narcisistic process.
[19] The barrier to automerisation of [*meso*]-**2**, via lone pair-lone pair passage through the intra-amine gap, is likely to be similar to that reported for the automerisation of **1** (ca. 7.5 kcal mol^{-1} − see R. W. Alder, J. E. Anderson, *J. Chem. Soc., Perkin Trans 2* **1973**, 2086−2088).
[20] R. W. Alder, M. R. Bryce, N. C. Goode, N. Miller, J. Owen, *J. Chem. Soc., Perkin Trans. 1* **1981**, 2840−2847.
[21] G. H. Coleman, C. R. Hauser, *J. Am. Chem. Soc.* **1928**, *50*, 1196.
[22] M. L. Kaplan, F. A. Bovey, H. N. Cheng, *Anal. Chem.* **1975**, *47*, 1703−1704; A. L. Van Geet, *Anal. Chem.* **1970**, *42*, 679−680

Received April 12, 1999
[O99206]